Molecular Mechanism of Lateral Diffusion of py_{10}-PC and Free Pyrene in Fluid DMPC Bilayers

Jorge Martins* and Eurico Melo*†
*Instituto de Tecnologia Química e Biológica-UNL, Oeiras, Portugal, and †Instituto Superior Técnico, Lisboa, Portugal

ABSTRACT From the study of the kinetics of the fluorescence self-quenching of pyrene in multilamellar vesicles of 1,2-dimyristoyl-*sn*-glycero-3-phosphocholine (DMPC) in the fluid phase we obtain the molecular diffusion parameters, diffusion coefficients, and activation energies for lateral diffusion for three probes: 1-palmitoyl-2-(1-pyrenedecanoyl)-*sn*-glycero-3-phosphocholine (py_{10}-PC), pyrene, and 1-pyrenebutanoic acid (py-but). The experiments are done in a range of temperatures for which the reversibility of excimer formation is negligible and the probe/phospholipid ratios used are low, avoiding non-ideal mixing of the probe. The time-resolved fluorescence decays are, in all cases, accurately and consistently described by the two-dimensional (2D) formalism for bimolecular diffusion-controlled reactions. From the parameters obtained in this way we conclude that the primary step of the diffusion of the pyrene-labeled phospholipid involves the simultaneous jump of phospholipid and fluorophore moieties, and also that although in the case of py_{10}-PC the pyrene from molecules pertaining to different layers may interact during the lifetime of the exited state, this is not the case for free pyrene.

INTRODUCTION

The theory of lateral diffusion in phospholipid bilayers has been the subject of much research (Clegg and Vaz, 1985). However, there are still unexplored aspects, namely those concerning the molecular mechanism of diffusion. The molecular diffusion parameters can be easily obtained from the analysis of the kinetics of diffusion-controlled reactions. Geometrically confined diffusion-limited reactions have low dimensional or fractal kinetics that differ drastically from a classical three-dimensional (3D) kinetics (Kopelman, 1989). In a diffusion-limited reaction the diffusive step leading to the encounter of reactants is the rate-limiting process, and classical diffusion-controlled reaction rate theory for 3D predicts that in these reactions the rate coefficient is time-dependent and independent on concentration (Rice, 1985). However, although in 3D the rate coefficient tends asymptotically to a constant value, the rate coefficient in 2D tends to zero at long times. The formalism for 2D diffusion-controlled kinetics was introduced by Razi Naqvi (1974), and we have proved that, in the case of 1-palmitoyl-2-(1-pyrenedecanoyl)-*sn*-glycero-3-phosphocholine (py_{10}-PC) in fluid 1-palmitoyl-2-oleoyl-*sn*-glycero-3-phosphocholine (POPC) bilayers, this formalism conduces to a self-consistent kinetic analysis of pyrene monomer and excimer fluorescence (Martins et al., 1996). Moreover, we have also shown that, whatever the time range considered, and for a large range of diffusion coefficients, encounter distances, and 2D concentrations, Razi Naqvi's formalism is in perfect accordance with the results of the simulation of 2D bimolecular reactions using Monte Carlo techniques (Martins et al., 2000).

In the present work we analyze and compare the kinetics of the diffusion-controlled self-quenching of free pyrene and py_{10}-PC in 1,2-dimyristoyl-*sn*-glycero-3-phosphocholine (DMPC) bilayers and discuss the results in terms of the mechanism and dynamics of molecular diffusion in fluid bilayers. The analysis of the fluorescence decays is done using the expression for the time-dependent bimolecular rate coefficient in circular geometry as a function of the molecular parameters: D_{eff} (the mutual diffusion coefficient) and R_C (the encounter distance),

$$k_{\text{diff}}(t) = \frac{8D_{\text{eff}}N_A}{\pi}\int_0^{\infty}\frac{\exp(-\alpha\beta^2)}{\beta[J_0^2(\beta) + Y_0^2(\beta)]}d\beta \qquad (1)$$

where $\alpha = D_{\text{eff}}t/R_C^2$, $J_0(\beta)$ and $Y_0(\beta)$ are the zero-order Bessel functions of the first and second kind, respectively, N_A is the Avogadro constant, and β is a dummy integration variable.

When using the method of time-correlated single photon counting in the case where the excitation cannot be considered a Dirac pulse, the experimentally obtained time-dependence of pyrene monomer fluorescence emission with bimolecular quenching, $I_M(t)$, is the convolution of the lamp profile, $L(t)$, with the monomer decay law. The decay law includes an emission term, τ_M (the pyrene monomer lifetime) plus a reaction term depending on $k_{\text{diff}}(\zeta)$ given by Eq. 1. Therefore, the experimentally observed fluorescence intensity decay is described by the following equation:

$$I_M(t) = L(t) \otimes \exp\left\{-\left(\frac{t}{\tau_M} + \int_0^t k_{\text{diff}}(\zeta)[M]d\zeta\right)\right\} \qquad (2)$$

where $\otimes$ denotes the convolution integral. The value of D_{eff} is obtained from the deconvolution analysis of the monomer

Received for publication 13 September 1999 and in final form 11 October 2000.

Address reprint requests to Eurico Melo, Instituto de Tecnologia Química e Biológica, ITQB-UNL, Av. da República, Apartado 127, P-2781-901 Oeiras, Portugal. Tel.: +351-214-469-724; Fax: +351-214-411-277; E-mail: eurico@itqb.unl.pt.

0006-3495/01/02/832/09 $2.00

decay using τ_M obtained for infinite dilution and R_C derived from the combined van der Waals radii (Edward, 1970). The concentration is expressed in 2D units (mol cm^{-2}).

Pyrene probes are used extensively in model membrane studies, mostly with the objective of obtaining lateral diffusion coefficients, but also to access phenomena such as interbilayer lipid transfer, lateral lipid organization, and mechanism of phospholipase action (Kinnunen et al., 1993). The depth at which the pyrenyl moieties of phospholipid probes or the free pyrene reside in the bilayer and the way in which the probe interacts with the bilayer molecular structure largely affect the interpretation given to the experimental results. This is of critical importance for the case of 2D kinetic studies.

It was suggested, based on a qualitative reasoning, that py_{10}-PC in DMPC bilayers are positioned such that excimer formation between pyrenyl groups belonging to different monolayers can take place (Hresko et al., 1986; Sugár et al., 1991). If so, this should imply that the effective 2D quencher concentration is doubled with respect to the case where the reaction takes place independently in each leaflet. We have proved in a previous work (Martins et al., 1996) that in fluid bilayers of POPC the pyrene moiety of probes pertaining to different sides can in fact interact, because only on this condition the parameters retrieved, namely τ_M, from the analysis with the 2D formalism have physical meaning. This is apparently inconsistent with the value of 1.11 nm for the depth of the effective center of the pyrenyl moiety of py_{10}-PC measured from the bilayer/water interface in POPC bilayers quoted by Sassaroli et al. (1995). However, this value is based on calculations considering that the phospholipid chains are in the random fluid conformation, which is not the case for the acyl chains in a bilayer (Seelig and Seelig, 1980; Trouard et al., 1999). Due to the profile of the order parameters of the acyl segments across a phospholipid bilayer this value is underestimated by ~0.3 nm. In the fluid phase the average length of the decanoyl segment is ≈1.0 nm (Cevc and Marsh, 1987), and the carbon C10 of the pyrenyl group is at ≈0.4 nm from the center of the ring system, resulting in a location for pyrene near the center of the bilayer (Martins et al., 1996). The fully extended length of the pyrenedecanoyl chain, from the carbon C1 to the hydrogen connected to C6 of the pyrenyl group, is ~1.99 nm, which compares with the maximum length of the myristoyl chain in the all-*trans* configuration, ~1.75 nm (Cevc and Marsh, 1987). However, in the fluid phase, due to the torsional freedom of the chains, the experimental hydrophobic length of DMPC multibilayers is ~1.3 nm (Petrache et al., 1998), while in the functionalized probe, due to the constant contribution of the rigid pyrene to the length of the pyrenedecanoyl chain, the pyrenyl group can surpass the center of the DMPC bilayer protruding into the opposing leaflet.

The free molecular pyrene is quite hydrophobic and barely soluble in water (solubility lower than 10^{-6} M). Therefore, in aqueous suspensions of liposomes it is trapped into the hydrocarbon region of the bilayer. This notion led to the argument that it is not an adequate model system for studies of 2D reactions because a free pyrene molecule could move in all directions inside the bilayer, resulting in a non-ideal 2D system (Almgren, 1991). The work of Podo and Blasie (1977), using ^{1}H-NMR to determine the relative positions of small aromatic molecules such as pyrene inside the bilayer, is not totally conclusive in this particular point. The ring current effect induced by free pyrene in the methylenic protons of 1,2-dipalmitoyl-*sn*-glycero-3-phosphocholine (DPPC) vesicles was found to be negligible at the level of the terminal methyl group, the effects being more significant in carbons 4 to 13. Podo and Blasie interpreted their observations as resulting either from a more rapid relative motion of the probe and/or alkyl chains near the center of the bilayer, or from a much lower probe occupancy at this depth. It is to be noted that the longest dimension of the pyrene molecule is 0.92 nm (Birks, 1970), which fits the ordered region of a saturated phospholipid bilayer. Molecular dynamics simulations, supported by independent experimental evidence, suggest that small solutes prefer to align their principal long axis along the bilayer normal (Xiang and Anderson, 1998). In the present work we discuss these two different possible probe distributions based on the analysis of the decays of self-quenching with the 2D kinetic model.

We use DMPC bilayers because of the convenient range of temperature in which they remain fluid, allowing the determination of the activation energy for diffusion in a region where the reversibility of the pyrene excimer is still negligible. All the needed structural parameters for the fluid DMPC bilayer are available in the literature: the monolayer hydrophobic thickness is 1.31 nm (Petrache et al., 1998) and the molecular area as a function of temperature has been calculated (Almeida et al., 1992). The reliability of the method used for the calculation of the molecular areas as a function of temperature is supported by the good accordance with the experimental value of 0.597 nm^2 for DMPC fluid bilayers at 30°C (Petrache et al., 1998).

Using the method previously delineated we retrieve the molecular lateral diffusion coefficient of free pyrene, py_{10}-PC, and py-but. The influence of the bilayer structure on the diffusion of py_{10}-PC is analyzed by comparing the present results in DMPC with our previous data in POPC. The diffusion coefficients obtained for this bulky group inside the bilayer are compared to the available data from FRAP (fluorescence recovery after photobleaching) and discussed in view of the different characteristics of the diffusing molecules. In addition to this analysis of the lateral diffusion mechanism, we also examine the validity of the pure 2D diffusion-controlled kinetic formalism, already validated for py_{10}-PC/POPC (Martins et al., 1996) for excimer formation between free pyrene molecules in DMPC fluid bilayers.

MATERIALS AND METHODS

Materials

The probe py-but was purchased from Molecular Probes (Eugene, OR) and used as received. Pyrene-labeled phospholipid py_{10}-PC from the same source required purification by HPLC. Zone-refined pyrene was a gift from Prof. J. M. G. Martinho (IST-UTL, Lisboa, Portugal). DMPC from Avanti Polar Lipids (Birmingham, AL), had its purity checked by HPLC and was used as received. All organic solvents were spectroscopic or HPLC grade from Merck (Darmstad, Germany) or Riedel-deHaën (Seelze, Germany). For all aqueous solutions and suspensions, a pH = 7.0 and 0.01 M phosphate (Merck, P.A.) buffer in Millipore Q water was used.

Liposome suspensions

Multilamellar liposomes were prepared by mechanical dispersion in buffer of the lipid film obtained removing the solvent (chloroform/methanol 2:1) of a solution of probe and phospholipid (2 h at 10^{-3} atm). The liposome suspension was centrifuged (12,000 × *g*, 10 min) and the pellet resuspended in buffer solution. The procedure was repeated twice, obtaining a final suspension ~0.3 mM in phospholipid. The concentrations of the stock solutions of pyrene, py_{10}-PC, and py-but were determined by UV/Vis absorption ($\epsilon_{334\ nm}$(pyrene) = 5.5 × 10^4 M^{-1} cm^{-1}, $\epsilon_{342\ nm}$(py_{10}-PC) = 4.2 × 10^4 M^{-1} cm^{-1}, and $\epsilon_{341\ nm}$(py-but) = 4.3 × 10^4 M^{-1} cm^{-1}, in ethanol). The final concentrations of DMPC, pyrene, py-but, and py_{10}-PC in the preparations were checked by HPLC (Merck-Hitachi with LiChroCART RP18 columns). Probes and phospholipid concentrations in final suspensions were found to be within 3 to 9% of their intended values. All liposome solutions were maintained in an argon atmosphere in the dark at 4°C, and were measured within 48 h of preparation.

Spectroscopic measurements

Absorption spectra in the UV/Vis range were obtained with a Beckman DU-70 spectrophotometer. Corrected emission and excitation fluorescence spectra were determined with a SPEX Fluorolog 212I spectrofluorimeter. Time-resolved fluorescence determinations were performed by conventional time-correlated single photon counting, using an apparatus described elsewhere (Maçanita et al., 1989; Martins et al., 1996). The samples were excited with the 337-nm line of the pulsed nitrogen lamp, corresponding to the pyrene $S_2 \leftarrow S_0$ absorption transition. Monomer emission was collected at 376 nm in the cases of py_{10}-PC and py-but, and 373 nm for molecular pyrene, using appropriate cutoff filters to eliminate scatter from liposome suspensions. All decays have at least 2 × 10^4 counts at the maximum of the decay curve except for single-exponential decays, for which 10^4 counts are sufficient. The samples were continuously stirred during measurements and the temperature controlled to ±0.5°C after a stabilization period of 10 min. Samples were degassed with 10 argon-low vacuum cycles (without freezing) and the fluorescence cell closed with a Teflon stopper.

Fluorescence decay analysis

Fluorescence decay and its analysis were described in a previous paper (Martins et al., 1996). In that paper the experimental details, the methods of monomer (and excimer) decay analysis, and the justification for the necessity of the 2D kinetic formalism for the interpretation of py_{10}-PC probe excimer formation kinetics in fluid POPC are extensively described and discussed. A brief summary of the method used is given below.

For very low probe concentration (probe/lipid ratio lower than 1:1500) no self-quenching is observed, and a single-exponential law convoluted with the experimental lamp profile is fitted to the data. As usual, the pre-exponential and the unquenched fluorescence lifetime, τ_M, are obtained. The value of the mutual diffusion coefficient, D_{eff}, is determined from the kinetics of self-quenching at a concentration high enough for ensuring an accurate determination, but not so high that it results in non-ideal mixing of the probe (probe/lipid ratio lower than 1:75). For D_{eff} retrieval both 2D and 3D formalisms were used. When a 2D analysis is envisaged Eq. 2 is fitted to the experimental decay. In the case where the reactional space is treated as 3D medium, the convoluted decay is analyzed using Eq. 3 (Nemzek and Ware, 1975).

$$I_M(t) = L(t) \otimes \exp\left\{ -\left(\frac{1}{\tau_M} + \frac{4\pi R_C D_{eff} N_A[M]}{1000}\right)t - \left(\frac{8R_C^2\sqrt{\pi D_{eff}}N_A[M]}{1000}\right)\sqrt{t}\right\} \quad (3)$$

In this equation the 3D concentration (in mol dm^{-3} units) is calculated considering all the volume of the hydrophobic core of DMPC bilayers as the reaction compartment, that is, considering a 3D isotropic medium where the reactants are free to diffuse. It is important to point out that although in both 2D and 3D cases we should fix τ_M, leaving the pre-exponential and D_{eff} free to be adjusted, the deconvolution was always performed without forcing τ_M to allow for small differences in the degassing conditions. The value of R_C = 0.71 nm (R_{Py} = 0.356 nm) is calculated by the theory of Edward (1970), and the molar concentration in 2D (in mol cm^{-2} units) corrected for the thermal expansion of DMPC bilayers (Almeida et al., 1992).

All calculations were performed in a personal computer using FORTRAN routines (Chandler, 1976; Press et al., 1992; Martins et al., 1996).

RESULTS AND DISCUSSION

Lifetimes in the absence of self-quenching

The fluorescence decay of pyrene probes, pyrene, py-but, and py_{10}-PC dissolved in pure DMPC multilamellar liposomes was obtained for temperatures in the 25–45°C range. At and above 25°C the phospholipid bilayer is in the L_α fluid phase (T_m = 24.1°C (Marsh, 1990)) but at temperatures higher than 45°C the significant reversibility of the pyrene excimer (Duveneck, 1986) is an inconvenience for the kinetic analysis to be performed in the next section (Martins et al., 1996). The fluorescence decay of the free pyrene monomer in DMPC liposomes, for a probe to lipid ratio of 1:2000 at 30°C, is shown in Fig. 1 together with the result from single-exponential deconvolution. When using low concentrations, probe to lipid ratio lower than 1:1500, the fluorescence decays of all the probes are perfectly described by a single exponential law (as judged by the retrieved statistical parameters, as well as by weighted residuals and autocorrelation analysis). The monomer lifetimes in the absence of self-quenching, τ_M, as a function of temperature, obtained by averaging over several measurements, are presented in Table 1. The dispersion of lifetimes obtained for independent measurements is small, confirming that our degassing procedure provides quite reproducible oxygen concentrations. Given the degassing conditions and the environment of the chromophore, the values obtained are the ones expected and in accordance with those existing in the literature. The mean values of τ_M, show a small systematic decrease with increasing temperature.

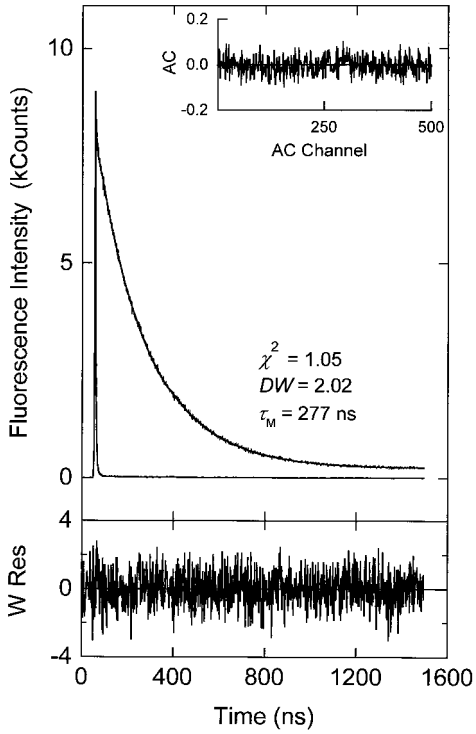

FIGURE 1 Lamp profile, calculated convoluted curve, and fluorescence decay of molecular pyrene in MLV of DMPC, collected at 373 nm and at T = 30°C, for a probe/phospholipid ratio of 1:2000. The presented weighted residuals (W Res) and autocorrelation function (A C) are the results of the deconvolution with a single-exponential law, with τ_M = 277 ns. The goodness-of-fit parameters χ^2 and DW are also shown.

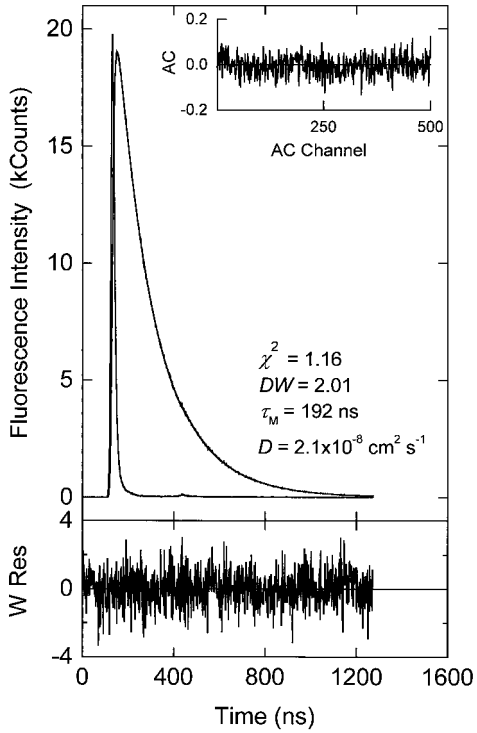

FIGURE 2 Lamp profile and fluorescence decay of py_{10}-PC in MLV of DMPC, at 376 nm and T = 30°C, for a probe/phospholipid ratio of 1:100. Also plotted is the convoluted curve, calculated from Eq. 2, and as the weighted residuals and the autocorrelation function. The fitting parameters, τ_M and D, and goodness-of-fit parameters, χ^2 and DW, are also presented.

Diffusion-controlled self-quenching of py_{10}-PC

In Fig. 2 the experimental fluorescence decay of py_{10}-PC monomer for a probe/phospholipid ratio of 1:100 at 30°C is depicted together with the fitted decay calculated by convolution with the experimental lamp profile, also shown, with the theoretical decay (Eq. 2). In the same figure we also present the retrieved fit parameters and the goodness-of-fit indicators, χ^2 and DW, and the plots of the weighted residuals and autocorrelation function. As already mentioned, these calculations are made considering interaction between pyrenyl groups pertaining to apposed monolayers. It is evident from the distribution of the residuals and autocorrelation values that the experimental decay is described accurately by the formalism of Razi Naqvi. At a given temperature the molecular diffusion coefficients obtained are identical, within the experimental error, irrespective of the molar py_{10}-PC to phospholipid ratio used (data not shown). This independence of the molecular diffusion coefficient, D ($D = D_{eff}/2$) on concentration was previously demonstrated for py_{10}-PC in POPC bilayers, and it was additionally shown that the same value can be obtained from the analysis of the excimer time-dependent emission profile or from steady-state data (Martins et al., 1996). The recovered values for D as a function of temperature are presented in Table 2. In the same table we also show the values of the unquenched lifetime, τ_M, retrieved from the fit of Eq. 2 (see Materials and Methods for details on fluorescence decay analysis). The values of τ_M obtained from the decays with self-quenching are coherent with those obtained directly from the diluted samples (Table 1). The recovered values for D reflect the expected increase of molecular mobility as a function of temperature. Again, the independence of D and τ_M on reactant concentration is itself a confirmation of the suitability of the 2D formalism to describe this kinetics.

TABLE 1 Fluorescence lifetimes, τ_M, of pyrene, py_{10}-PC, and py-but monomers at low concentration, obtained from the single-exponential analysis of the experimental decays, for different temperatures. The presented values were averaged over at least three experimental decays

	τ_M (ns)		
T (°C)	Pyrene	py_{10}-PC	py-but
25	272 ± 6	210 ± 5	204 ± 4
30	268 ± 5	206 ± 5	
35	263 ± 6	201 ± 7	197 ± 5
40	256 ± 8	195 ± 7	
45	250 ± 9	189 ± 8	

TABLE 2 Lateral diffusion coefficients, D, and unquenched lifetimes, τ_M, retrieved from the analysis with Eq. 2 of the fluorescence decays of pyrene, py_{10}-PC, and py-but monomers, for several temperatures. The parameters result from the analysis averaged from at least five decays.

	Pyrene		py_{10}-PC		py-but	
T (°C)	D (10^{-8} cm^2 s^{-1})	τ_M (ns)	D (10^{-8} cm^2 s^{-1})	τ_M (ns)	D (10^{-8} cm^2 s^{-1})	τ_M (ns)
25	6.4 ± 0.3	266 ± 4	1.1 ± 0.5	197 ± 5	6.7 ± 0.4	198 ± 5
30	7.5 ± 0.5	263 ± 5	2.1 ± 0.4	191 ± 4		
35	9.4 ± 0.7	261 ± 5	3.0 ± 0.7	190 ± 6	8.9 ± 0.5	195 ± 6
40	12 ± 0.6	257 ± 8	4.3 ± 0.8	187 ± 7		
45	14 ± 0.9	252 ± 7	6.2 ± 0.8	186 ± 8		

What if we consider that reaction between probes pertaining to different leaflets is not possible? In this case the fits obtained are also very good; the D values are only marginally higher, but the values of τ_M are systematically ~15% lower than those obtained for the very dilute system. Therefore, the coherence found when considering reaction between probes pertaining to different leaflets is lost. In the Introduction we have presented structural reasons for the interaction of probes from apposed leaflets, a hypotheses that is now experimentally confirmed.

From the slope of the Arrhenius type plot of $\ln(D/T)$ versus $1/T$ between 30 and 45°C, we calculate the activation energy for lateral diffusion, $E_a = 58(\pm 3)$ kJ mol^{-1}. At 25°C a value of D out of correlation (lower than expected) was obtained which may be attributed to either a larger uncertainty in the temperature or the proximity of T_m.

The D and E_a values for py_{10}-PC in DMPC bilayers are to be compared with those obtained from FRAP for NBD-DMPE, *N*-(7-nitrobenz-2-oxa-1,3-diazol-4-yl)-1,2-dimyristoyl-*sn*-glycero-3-phosphoethanolamine, in the same phospholipid matrix. For the same temperature our D values are two to three times lower than those for NBD-DMPE in DMPC, e.g., at 30°C $D = 5.9 \times 10^{-8}$ cm^2 s^{-1} (Vaz et al., 1985a). Our value of E_a is also roughly a factor of two higher than the value of E_a of NBD-DMPE in DMPC (corrected for the kinetic energy of the probe in the temperature range used, ≅2.5 kJ mol^{-1}, it is 30.5 kJ mol^{-1}). The referred difference in D cannot be attributed to a mass effect (Alder et al., 1974) because the two probes, NBD-DMPE and py_{10}-PC, have a similar molar mass: 850 g/mol for py_{10}-PC and ~800 g/mol for NBD-DMPE, the molar mass of DMPC being 678 g/mol. Another reason for the lower D values and higher E_a for lateral diffusion could be the larger cross-sectional area of py_{10}-PC (Somerharju et al., 1985). The cross-sectional area of py_{10}-PC in monolayers was found to be ~10% larger (Somerharju et al., 1985) than that of egg phosphatidylcholine, hence we may expect the molecular area of py_{10}-PC to be ~0.76 nm^2, which is to be compared with that of DMPC, 0.597 nm^2 at 30°C (Petrache et al., 1998). However, NBD-labeled egg phosphatidylethanolamine has D values and E_a for diffusion in DMPC that do not significantly differ from those of NBD-DMPE in the same lipid (Clegg and Vaz, 1985). Assuming that the NBD label in the headgroup has only a minor effect for the diffusion process (Clegg and Vaz, 1985) it is clear that another reason, besides an increase in molecular area, has to be invoked to explain our results. The difference in the length of the hydrophobic chain should not in principle result in such large changes in the values of D and E_a. In fact, it is well known that the D values observed both for NBD-PE phospholipids and NBD-labeled isoprenoid alcohols in a given phospholipid matrix are independent of the probe molecule chain length (Vaz et al., 1985a; Balcom and Petersen, 1993), the same being the case with E_a. Therefore, no difference is to be expected due to the fact that py_{10}-PC is longer than the C14 chains of the phospholipid matrix. Other possible contributing factors to the small D and high E_a that must be analyzed are the effect of the protrusion of the longer pyrenedecanoyl chain (and rigid pyrenyl group) into the apposed leaflet and the restriction of the intramolecular torsional freedom of the decanoyl chain due to the "anchor" effect exerted by the pyrenyl group. The fact that an independent cavity in the apposed leaflet is also needed for an effective diffusion step to take place may reduce the D values, but does not affect the E_a for the diffusion process, as has been clearly demonstrated using membrane-spanning labeled lipids by Vaz et al. (1985b). The second factor, the hindering of the decanoyl chain dynamics, cannot be ruled out but there is no experimental evidence giving support to it.

We are forced to conclude that a difference must exist between the molecular mechanism of the diffusion of an NBD-labeled phospholipid and py_{10}-PC. It was demonstrated that in the case of NBD-PE probes the lateral diffusion coefficient and activation energy for diffusion are independent of the probe chain length and nearly independent of the hydrophobic length of the phospholipid matrix (Vaz et al., 1985a). Therefore, the cavity necessary for the diffusion process to take place is similar irrespective of the length of the probe and lipid hydrophobic chain. This may have two interpretations: either the volume of the cavity is that of the headgroup (including the rigid glycerol backbone), or it includes also the first part of the chains (~8 carbons) known to correspond to the plateau section of the segmental order parameter (Trouard et al., 1999). The data obtained by Vaz et. al. (1985b) with a membrane-spanning

NBD-labeled rigid probe, NBD-MSPE, allows distinguishing between these two mechanisms. The fact that the E_a for this probe is the same as NBD-POPE, but the D values only ~⅔ of those for NBD-POPE, has been interpreted as resulting from NBD-MSPE acting as a "stiff" rod with nonsimultaneous jump of each extremity. Then, for NBD-MSPE the cavity in each monolayer needs to accommodate the "stiff" rod. The identity of E_a implies that the cavity needed for a discrete diffusional jump is the same in both cases, therefore involving the simultaneous opening of the headgroups and adjacent ordered chain region as a block. The E_a of NBD-PE probes in several phosphatidylcholine bilayers is similar, not only because the headgroups are the same but also because the length of the ordered region is more or less the same. The portion of the probe chain immersed in the disordered bilayer region does not play any role in this step. In the case of py_{10}-PC the value of E_a indicates that a much larger cavity has to be opened in the primary step of diffusion. If we consider that the activation energy for diffusion of molecular pyrene in a viscous hydrocarbon, e.g., squalane, is 31 kJ mol^{-1} (Olea and Thomas, 1988) and that adding this energy to that for NBD-DMPE in DMPC we obtain 61.5 kJ mol^{-1}, very similar to what is obtained for py_{10}-PC in DMPC, we are led to conclude that the phospholipid and pyrene moieties of py_{10}-PC jump *simultaneously*. In Fig. 3 *a* we schematize this mechanistic interpretation of the molecular diffusion of an NBD-DMPE and of a py_{10}-PC molecule in a DMPC fluid bilayer. When the head + chain block of a DMPC molecule jumps, their tails are left behind. In the picture the ordered region is presented as consisting of 8 carbons and perfectly rigid, which may not be the case, but the idea is that a cavity must also be opened to accommodate the first 6–8 carbons. In the case of py_{10}-PC, the pyrenyl group cannot be left behind because this rigid group is closely attached to the ordered portion of the decanoyl chain. Again, the rigidity of the diffusing molecule may be exaggerated in the picture but it is clear from our data that a much larger cavity has to be opened.

Our previous results for the lateral diffusion of py_{10}-PC in POPC gave $D = 3.9 \times 10^{-8}$ cm^2 s^{-1} at 30°C, the activation energy for lateral diffusion being 35 kJ mol^{-1}. How can the interpretation given for the case of DMPC be consistent with our findings for the py_{10}-PC in POPC system where E_a is only 1.4 times higher than NBD-DSPE in POPC (identical to that of other NBD labeled probes with saturated chains in POPC (Vaz et al., 1985a))? Our interpretation is that in the case of POPC the pyrenyl group of py10-PC is not "forced" to diffuse simultaneously with the head block, as pictured in Fig. 3 *b*. The reason for this is, due to the *cis* double bond at C9 of the oleoyl chain in the *sn*-2 position, the segmental order of this chain is greatly lowered (Seelig and Seelig, 1980) and the pyrenedecanoyl chain (also in the *sn*-2 position of glycerol) can be left behind during the

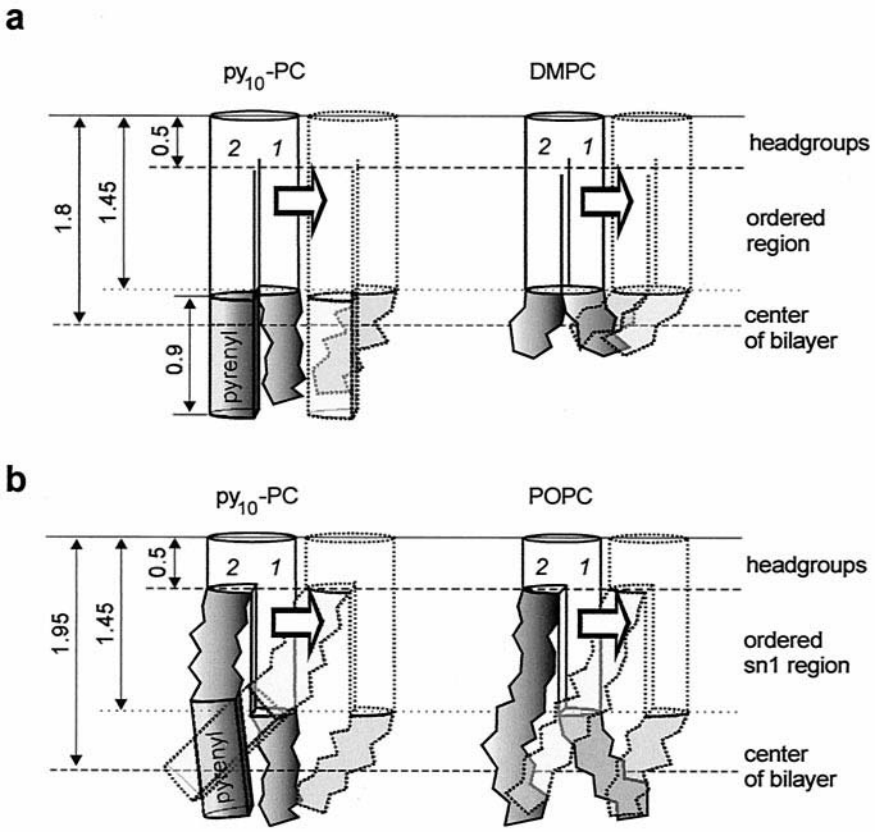

FIGURE 3 Schematic representation of the diffusion mechanism of py_{10}-PC and phospholipid in one monolayer from a DMPC (*a*) and a POPC (*b*) bilayer. The dimension captions are in nanometers and obtained from the references given in the text, the chains are numbered as 2 for *sn*-2 and 1 for *sn*-1. To simplify the drawing the length of a diffusional jump is represented as being equal to a phospholipid diameter, which is certainly not the case, and the number of carbons in a chain is not precisely given.

primary diffusional jump, as schematized in Fig. 3 *b*. This effect was already present in the case of the diffusion of NBD-labeled phospholipids that have an activation energy 20% lower in POPC than in DMPC, which we interpret as the result of the relative freedom of the *sn*-2 chain (see Fig. 3 *b*).

Diffusion-controlled self-quenching of free pyrene

Fluorescence decays of the free pyrene monomer for probe to lipid ratios 1:100 and 1:200 at 30°C are presented together with the fit to Eq. 2 in Fig. 4. The 2D concentration used in the analysis considers the pyrene intercalated in the palisade region of the bilayer, therefore supposing that there is no excimer formation between molecules located in apposed monolayers, an option that will be further discussed after the analysis of py-but data. For both probe/lipid ratios Eq. 2 describes the experimental decays with accuracy, the τ_M and D values obtained being identical within the experimental error. Also, τ_M for the several temperatures measured (Table 2) is identical, within the experimental error, to that obtained in the experiments without self-quenching (Table 1). The values and temperature-dependence of the diffusion coefficients (Table 2) follow the expected trend and can be rationalized, as will be discussed later.

The analysis with a 3D formalism does not allow retrieval of molecular parameters with physical significance. For instance, considering that the pyrene molecules are able to move in a 3D space inside the hydrophobic core, the same 1:100 decay at 30°C analyzed with the Smoluchowski 3D formalism (Fig. 5) gives $\tau_M = 451$ ns and $D = 7.9 \times 10^{-8}$ cm^2 s^{-1}, and for the 1:200 concentration at the same temperature, $\tau_M = 395$ ns and $D = 6.4 \times 10^{-8}$ cm^2 s^{-1}. Moreover, the τ_M and D values as a function of temperature do not change in a coherent way. It goes without saying that the excellent residuals and statistical parameters obtained in Fig. 5 result only from the similarity of the mathematical expression for the rate coefficient for 3D kinetics (Rice, 1985) with that of the series expansion of Eq. 1 for short times (Razi Naqvi, 1974). Therefore, no physical meaning can be attributed to the values of τ_M and D retrieved in this way.

In the 2D analysis we have considered the free pyrene confined to each monolayer. A subsequent confirmation that this is the case is obtained from the lack of consistence of the parameters retrieved by doubling the pyrene 2D concentration, that is, considering that all the pyrene molecules residing in the bilayer contribute to the self-quenching. Analyzed in this way, the τ_M values obtained are lower that those in the absence of self-quenching and do not follow the expected trend with temperature, the D values being lower and disperse.

An additional verification of the correctness of this approach has been done using the free pyrene analog py-but. At pH 7.0 the location of py-but in the DMPC bilayer is

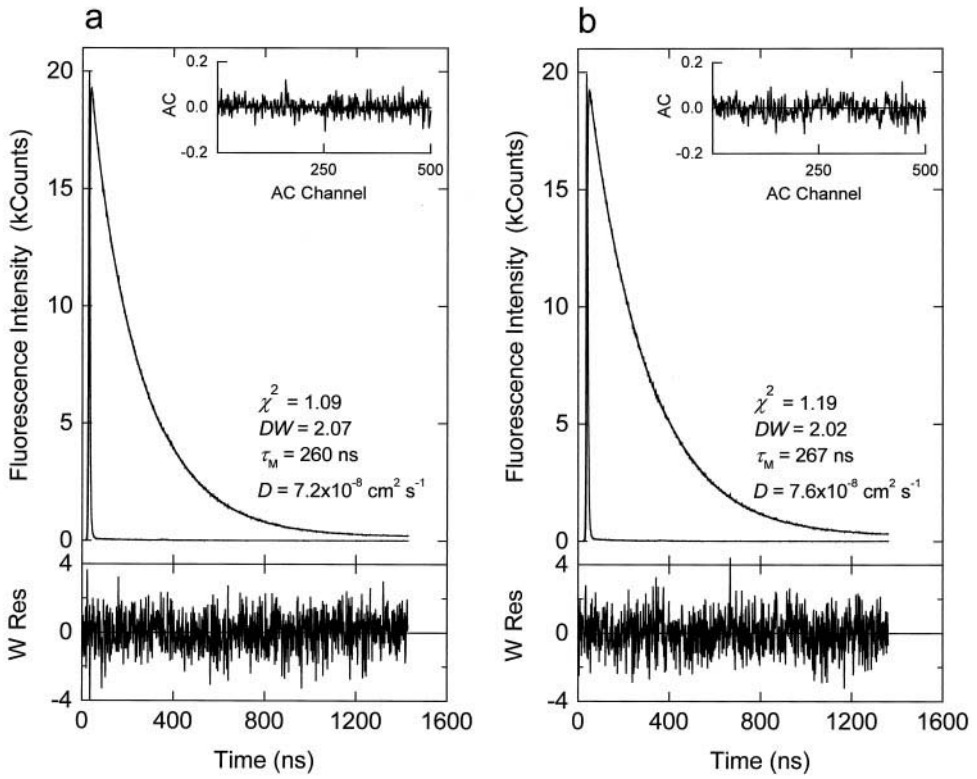

FIGURE 4 Lamp profile and fluorescence decay of free pyrene, at 373 nm, in MLV of DMPC at 30°C for a probe/phospholipid ratio of (*a*) 1:100 and (*b*) 1:200. Also plotted is the calculated convoluted curve with Eq. 2. For each case the weighted residuals and the autocorrelation function are shown, as well as the fitting parameters, τ_M and D, and the respective χ^2 and DW values.

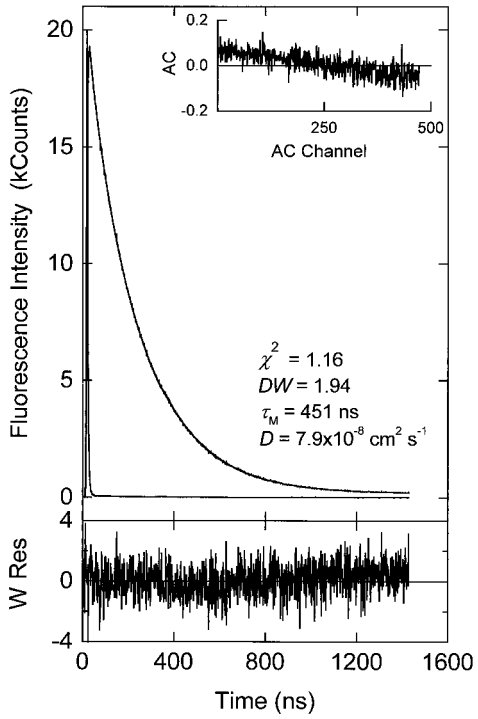

FIGURE 5 The same fluorescence decay presented in Fig. 4 *a* now analyzed with the Smoluchowski formalism, Eq. 3, together with the τ_M and D values obtained from the fit for which χ^2 and DW are also shown.

determined by the ionized carboxyl group. The deconvolution of the fluorescence decays with Eq. 2 is performed considering that due to the probe dimensions and anchoring at the interface there is only excimer formation for pyrenes pertaining to the same monolayer. At 25°C we obtain $D = 6.9(\pm0.4) \times 10^{-8}$ cm^2 s^{-1} and $\tau_M = 198(\pm5)$ ns, and at 35°C $D = 8.9(\pm0.5) \times 10^{-8}$ cm^2 s^{-1} and $\tau_M = 195(\pm6)$ ns (Table 2). The unquenched lifetime is typical of 1-pyrenyl derivatives and the D values are, within the experimental error, identical to those of free pyrene. These results do not add any new facts in what was already discussed concerning free pyrene, but strongly support our decision of using the two leaflets of the bilayer as two separate 2D reaction compartments.

The E_a for the lateral diffusion of molecular pyrene obtained from the slope of the Arrhenius-type plot for a temperature range between 25 and 45°C is 28(±4) kJ mol^{-1}. This E_a is, as already mentioned, about the same as that observed for free pyrene in viscous hydrocarbons, and also that expected for the opening of a cavity in the more ordered region of a DMPC bilayer. However, having already concluded that the pyrene molecules reside in the palisade region, this energy is the one involved in the diffusive step in the palisade region. The D values obtained by us are ~25% higher than those of NBD-DMPE in DMPC, and ~18% higher then those of isoprenoid alcohols also in DMPC (Vaz et al., 1985a; Balcom and Petersen, 1993). In these cases the diffusing molecule has a higher molecular mass than pyrene (MM = 202 g mol^{-1}) which may justify the differences observed. An unquestionable confirmation of the correctness of the diffusion coefficients obtained is encountered in the D values for polyaromatic hydrocarbons, tetracene (MM = 228 g mol^{-1}) and rubrene (MM = 533 g mol^{-1}), in DMPC bilayers at 29°C measured by FRAP: D(tetracene) = $1.1(\pm0.9) \times 10^{-7}$ cm^2 s^{-1} and D(rubrene) = $5.8(\pm0.3) \times 10^{-8}$ cm^2 s^{-1} (Balcom and Petersen, 1993).

CONCLUSIONS

The analysis of the diffusion-controlled reaction of pyrene excimer formation between the pyrenyl moieties of py$_{10}$-PC in fluid DMPC bilayers was shown to be correctly and coherently described by the Razi Naqvi formalism for reactions in pure 2D geometry, which is in accordance with our previous findings for the same probe in POPC (Martins et al., 1996). We have now demonstrated that free pyrene molecules in DMPC, despite being a less obvious 2D system, react with a kinetics perfectly described by the same formalism. The values of molecular diffusion coefficients we obtain have physical meaning, which is not the case when an analysis with the 3D Smoluchowski formalism is performed.

In the case of free pyrene, an analysis considering the pyrene located at the central region of the bilayer leads to incoherent results. Most probably the pyrene molecules are free to jump from one leaflet to the other, but within the lifetime of the excited pyrene monomer it may be considered confined to a single leaflet of a DMPC bilayer in the fluid phase.

Lateral diffusion of py$_{10}$-PC in DMPC is shown to take place in a single jump involving the opening of a cavity accommodating both phospholipid and fluorophore moieties. This does not seem to be the case in POPC where, due to the palisade region being less ordered, there is no need for a cavity accommodating the pyrenyl group for the primary step of diffusive motion to take place.

We thank Winchil L. C. Vaz for many useful discussions leading to the final version of this work.

The research described herein was partially supported by the program PRAXIS from FCT-Portugal. J.M. gratefully acknowledges JNICT-Portugal for Grant D/98/90-RM.

REFERENCES

Alder, B. J., W. E. Alley, and J. A. Dymond. 1974. Studies in molecular dynamics. XIV. Mass and size dependence of the binary diffusion coefficient. *J. Chem. Phys.* 61:1415–1420.

Almeida, P. F. F., W. L. C. Vaz, and T. E. Thompson. 1992. Lateral diffusion in the liquid phase of dimyristoylphosphatidylcholine/cholesterol lipid bilayers: a Free Volume analysis. *Biochemistry.* 31: 6739–6747.

Almgren, M. 1991. Kinetics of excited state processes in micellar media. *In* Kinetics and Catalysis in Microheterogeneous Systems. M. Grätzel and K. Kalyanasundaram, editors. Marcel Dekker, New York. 63–112.

Balcom, B. J., and N. O. Petersen. 1993. Lateral diffusion in model membranes is independent of the size of the hydrophobic region of molecules. *Biophys. J.* 65:630−637.

Birks, J. B. 1970. Photophysics of Aromatic Molecules. Wiley-Interscience, London.

Cevc, G., and D. Marsh. 1987. Phospholipid Bilayers: Physical Principles and Models. John Wiley and Sons, New York.

Chandler, J. P. 1976. QCPE Routines Packages: STEPT (QCMP037). Indiana University, Bloomington.

Clegg, R. M., and W. L. C. Vaz. 1985. Translational diffusion of proteins and lipids in lipid bilayer membranes. A comparison of experiments with theory. *In* Progress in Protein-Lipid Interactions, Vol. 1. A. Watts and J. J. H. H. M. De Pont, editors. Elsevier, Amsterdam. 173–229.

Duveneck, G. 1986. Ph.D. Kinetrische Untersuchungen an Diarylakanen thesis, Georg-August-Universität, Göttingen.

Edward, J. T. 1970. Molecular volumes and the Stokes-Einstein equation. *J. Chem. Ed.* 47:261–270.

Hresko, R. C., I. P. Sugár, Y. Barenholz, and T. E. Thompson. 1986. Lateral distribution of a pyrene-labeled phosphatidylcholine in phosphatidylcholine bilayers: fluorescence phase and modulation study. *Biochemistry.* 25:3813–3823.

Kinnunen, P. K. J., A. Kõiv, and P. Mustonen. 1993. Pyrene-labeled lipids as fluorescent probes in studies in biomembranes and membrane models. *In* Fluorescence Spectroscopy. O. S. Wolfbeis, editor. Springer-Verlag, Berlin. 159–169.

Kopelman, R. 1989. Diffusion-controlled reaction kinetics. *In* The Fractal Approach to Heterogeneous Chemistry: Surfaces, Colloids, Polymers. D. Avnir, editor. John Wiley and Sons, Chichester. 295–308.

Maçanita, A. L., F. P. Costa, S. M. B. Costa, E. Melo, and H. Santos. 1989. The 9-anthroate chromophore as a fluorescent probe for water. *J. Phys. Chem.* 93:336–343.

Marsh, D. 1990. Handbook of Lipid Bilayers. CRC Press, Boca Raton.

Martins, J., K. Razi Naqvi, and E. Melo. 2000. Kinetics of two-dimensional diffusion-controlled reactions: a Monte Carlo simulation of hard-disk reactants undergoing a Pearson-type random-walk. *J. Phys. Chem.* 104: 4986–4991.

Martins, J., W. L. C. Vaz, and E. Melo. 1996. Long-range diffusion coefficients in two-dimensional fluid media measured by the pyrene excimer reaction. *J. Phys. Chem.* 100:1889–1895.

Nemzek, T. L., and W. R. Ware. 1975. Kinetics of diffusion-controlled reactions: transient effects in fluorescence quenching. *J. Chem. Phys.* 62:477–489.

Olea, A. F., and J. K. Thomas. 1988. Rate constants for reactions in viscous media: correlation between the viscosity of the solvents and the rate constant of the diffusion-controlled reactions. *J. Am. Chem. Soc.* 110: 4494–4502.

Petrache, H. I., S. Tristam-Nagle, and J. F. Nagle. 1998. Fluid phase structure of EPC and DMPC bilayers. *Chem. Phys. Lipids.* 95:83–94.

Podo, F., and J. K. Blasie. 1977. Nuclear magnetic resonance studies of lecithin bimolecular leaflets with incorporated fluorescent probes. *Proc. Natl. Acad. Sci. U.S.A.* 74:1032–1036.

Press, W. H., B. P. Flannery, S. A. Teukolsky, and W. T. Wetterling. 1992. Numerical Recipes: The Art of Scientific Computing (FORTRAN Version), 2nd Ed. Cambridge University Press, Cambridge.

Razi Naqvi, K. 1974. Diffusion-controlled reactions in two-dimensional fluids: discussion of measurement of lateral diffusion of lipids in biological membranes. *Chem. Phys. Lett.* 28:280–284.

Rice, S. A. 1985. Diffusion-controlled reactions in solution. *In* Comprehensive Chemical Kinetics, Vol. 25. C. H. Bamford, C. F. H. Tipper, and R. G. Compton, editors. Elsevier, Amsterdam. 3–45.

Sassaroli, M., M. Ruonala, J. Virtanen, M. Vauhkonen, and P. Somerharju. 1995. Transversal distributions of acyl-linked pyrene moieties in liquid-crystalline phosphatidylcholine bilayers. A fluorescence quenching study. *Biochemistry.* 34:8843–8851.

Seelig, J., and A. Seelig. 1980. Lipid conformation in model membranes and biological membranes. *Q. Rev. Biophys.* 13:19–61.

Somerharju, P. J., J. A. Virtanen, K. K. Eklund, P. Vainio, and P. K. J. Kinnunen. 1985. 1-palmitoyl-2-pyrenedecanoyl glycerophospholipids as membrane probes: evidence for regular distribution in liquid-crystalline phosphatidylcholine bilayers. *Biochemistry.* 34:8843–8851.

Sugár, I. P., J. Zeng, and P. L.-G. Chong. 1991. Use of Fourier transforms in the analysis of fluorescence data. 3. Fluorescence of pyrene-labeled phosphatidylcholine in lipid bilayers membranes. A three-state model. *J. Phys. Chem.* 95:7524–7534.

Trouard, T. P., A. A. Nevzorov, T. M. Alam, C. Job, J. Zajicek, and M. F. Brown. 1999. Influence of cholesterol on dynamics of dimiristoylphosphatidylcholine as studied by deuterium NMR relaxation. *J. Chem. Phys.* 110:8802–8818.

Vaz, W. L. C., R. M. Clegg, and D. Hallmann. 1985a. Translational diffusion of lipids in liquid crystalline phase phosphatidylcholine multibilayers. A comparison of experiment with theory. *Biochemistry.* 24:781–786.

Vaz, W. L. C., D. Hallmann, R. M. Clegg, A. Gambacorta, and M. De Rosa. 1985b. A comparison of the translational diffusion of a normal and a membrane-spanning lipid in L_α phase 1-palmitoyl-2-oleoylphosphatidylcholine bilayers. *Eur. Biophys. J.* 12:19–24.

Xiang, T.-X., and B. D. Anderson. 1998. Influence of chain ordering on the selectivity of dipalmitoylphosphatidylcholine bilayer membranes for permeant size and shape. *Biophys. J.* 75:2658–2671.